Journal of Zhejiang University-SCIENCE A (Applied Physics & Engineering)
ISSN 1673-565X (Print); ISSN 1862-1775 (Online)
www.jzus.zju.edu.cn; www.springerlink.com
E-mail: jzus@zju.edu.cn

Design guidelines for fluid-elastic instability of tube bundles subjected to two-phase cross flow*

Ning SUN[1], Rui-jia CHENG[1], Ya-nan ZHANG[1], Bao-qing LIU[†‡1,2], Bengt SUNDEN[†‡2]

[1]*College of Energy Engineering, Zhejiang University, Hangzhou 310027, China*

[2]*Department of Energy Sciences, Lund University, SE-22100 Lund, Sweden*

[†]E-mail: baoqingliu@zju.edu.cn; Bengt.sunden@energy.lth.se

Received May 1, 2019; Revision accepted June 27, 2019; Crosschecked July 8, 2019

Abstract: Fluid-elastic instability of tube bundles is the main cause of vibration failure of heat exchangers. To establish more reasonable and reliable design guidelines for fluid-elastic instability of tube bundles subjected to two-phase cross flow, we investigated experimentally the effects of the flow conditions of the two-phase flow and the geometrical characteristics of the tube bundles on damping, vibration, and fluid-elastic instability. Moreover, we proposed recommended values of the instability constant based on the conductivity difference measurement (CDM) model and the classification of tube bundle arrangements. The reliability of these values was also verified. The results indicated that the damping ratio in the lift direction was smaller than that in the drag direction and fluid-elastic instability was more prone to occur. The order of stability of the four tube bundle arrangements from high to low was normal triangular, normal square, rotated square, and rotated triangular. Thus, to avoid fluid-elastic instability, the normal triangular tube bundle is recommended for large shell-and-tube heat exchangers subjected to two-phase cross flow. In addition, for normal square and normal triangular tube bundles, the recommended instability constant is 4.0. For rotated square and rotated triangular tube bundles, the recommended instability constant is 1.1 when the mass damping parameter is less than or equal to 0.54, otherwise the value is 1.5.

Key words: Tube bundle; Fluid-elastic instability; Two-phase cross flow; Design guidelines
https://doi.org/10.1631/jzus.A1900129 **CLC number:** TE965; TK172

1 Introduction

Shell-and-tube heat exchangers have a wide application in chemical, petrochemical, nuclear, metallurgical, and pharmaceutical industries. Presently, the damage to tube bundles caused by flow-induced vibration is one of the principal reasons for the failure of shell-and-tube heat exchangers. Generally, there are four main mechanisms of flow-induced vibration: turbulent buffeting, fluid-elastic instability, vortex shedding, and acoustic resonance, among which fluid-elastic instability is the most destructive (Weaver and Fitzpatrick, 1988; Desai and Pavitran, 2018). Design guidelines for the vibration of tube bundles induced by single-phase cross flows have been proposed (Pettigrew and Taylor, 1991; Liu LY et al., 2018). However, vibration of tube bundles induced by two-phase cross flows is also common in heat exchangers such as steam generators and condensers. Such vibration is more complex than that induced by single-phase cross flows, since it is not only closely related to the mixture characteristics and flow pattern, but also an additional parameter, the volumetric void fraction, is important. Therefore, the study of the fluid-elastic instability of tube bundles subjected to two-phase cross flows is of great practical significance.

‡ Corresponding author

* Project supported by the National Natural Science Foundation of China (No. 21776246), the Fundamental Research Funds for the Central Universities (No. 2019QNA4020), China, and the China Scholarship Program (No. 201806325014)

ORCID: Bao-qing LIU, https://orcid.org/0000-0002-3393-1309

There have been some reports on the fluid-elastic instability of tube bundles subjected to two-phase cross flows. Moran and Weaver (2013) and Álvarez-Briceño et al. (2017) studied the damping of tube bundles in a two-phase cross flow. Pettigrew et al. (1995) and Violette et al. (2006) investigated the fluid-elastic instability of tube bundles in the lift and drag directions, and discussed the influence of the arrangement of rigid and flexible tubes on fluid-elastic instability. In air-water two-phase flow, Violette et al. (2006) and Ricciardi et al. (2011) investigated the vibration characteristics of tube bundles with different void fractions, while Pettigrew et al. (1989b) and Chung and Chu (2005) studied the effects of the geometrical characteristics of tube bundles on fluid-elastic instability. Álvarez-Briceño et al. (2018) proposed a method for the prediction of tube displacement amplitude based on a thorough consideration of the void fraction, mass flux, and flow pattern. The goal of fluid-elastic instability research is to obtain design guidelines for practical engineering applications. On the basis of the empirical correlation recommended by Connors (1970), some studies have proposed design guidelines according to stability maps, which consist of dimensionless velocity and mass damping parameters (Liu BQ et al., 2018). The Connors correlation is as follows:

$$\frac{V_{\mathrm{cr}}}{f_{\mathrm{n}}d}=K\left(\frac{2\pi m\zeta}{\rho d^{2}}\right)^{n}, \tag{1}$$

where V_{cr} is the critical velocity, f_{n} is the natural frequency of the tube in air, d is the outer diameter of the tube, $V_{\mathrm{cr}}/(f_{\mathrm{n}}d)$ is the dimensionless velocity, K is the instability constant, m is the mass per unit length including hydrodynamic mass, ζ is the damping ratio, ρ is the homogeneous density of the two-phase cross flow, n is the exponential constant, and $2\pi m\zeta/(\rho d^{2})$ is the mass damping parameter. Based on Connors correlation, Pettigrew et al. (2001) suggested formulas to calculate the instability constant K, which were suitable for various bundles, as follows:

$$K=3,\quad p/d\geq 1.47, \tag{2a}$$

$$K=4.76\left(p-d\right)/d+0.76,\quad 1.22\leq p/d<1.47, \tag{2b}$$

where p is the pitch between tubes, and p/d is the pitch-to-diameter ratio. The above formulas have been adopted by many researchers. However, Mitra et al. (2009) found that the actual instability constant of a normal square tube bundle with a pitch-to-diameter ratio of 1.4 in an air-water cross flow was 6.2, which is significantly different from the value predicted by Eq. (2). Actually, it is unreasonable to determine the instability constant only from the pitch-to-diameter ratio, since the tube bundle arrangement is an important factor affecting fluid-elastic instability which should also be taken into account.

For this reason, the effects of void fraction, pitch-to-diameter ratio, and tube bundle arrangement on fluid-elastic instability were thoroughly investigated in this study. Based on our experimental results, we proposed recommended instability constants of the fluid-elastic instability of tube bundles induced by two-phase cross flows.

2 Experiment

2.1 Experimental apparatus

The experimental apparatus (Fig. 1) was composed of an inlet chamber, test chamber, outlet chamber, static-dynamic strain gauge, and dual conductivity probe. Specifications of major experimental instruments and equipment used in this study are provided in Table 1. The test chamber was equipped with experimental tube bundles whose structures are shown in Fig. 2. To obtain fully developed two-phase flow, a mixer was installed at the upper end and a gas distributor at the lower end of the inlet chamber. The gas transported by the compressor entered the inlet chamber from the bottom, and then flowed through the gas distributor and mixer in sequence, while the water in the tank was pumped directly to the mixer. The gas phase and liquid phase were thoroughly mixed in the mixer, then flowed into the test chamber and the outlet chamber in turn, and finally returned to the tank. Considering the difficulty and high cost of steam-water two-phase flow experiments, an air-water mixture was selected as the experimental medium. Axisa et al. (1984) found that the instability constants obtained in air-water and steam-water cross flows were almost equal, which indicates that it is feasible to use air-water instead of steam-water to study the fluid-elastic instability of tube bundles.

Table 1 Major experimental equipment and instruments

Name	Specification	Range	Accuracy
Centrifugal pump	MHF-6AR	12–72 m^3/h	–
Air compressor	W-0.8/12.5	0–48 m^3/h	–
Electromagnetic flowmeter	LDG-MK	2–85 m^3/h	±0.5%
Rotor flowmeter	LZB-15, LZB-25	0.4–4 m^3/h, 2.5–25 m^3/h	±2.5%
Static-dynamic strain gauge	TST3827	0–3000 με, 0–30000 με	±0.5%
Dual conductivity probe	BVW-2	0–50%	±0.5%

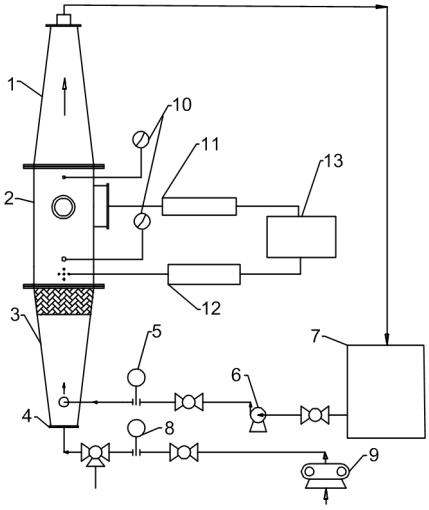

Fig. 1 Experimental apparatus

1: outlet chamber; 2: test chamber; 3: inlet chamber; 4: gas distributor; 5: electromagnetic flowmeter; 6: centrifugal pump; 7: storage tank; 8: rotor flowmeter; 9: air compressor; 10: pressure gauge; 11: static-dynamic strain gauge; 12: dual conductivity probe; 13: computer

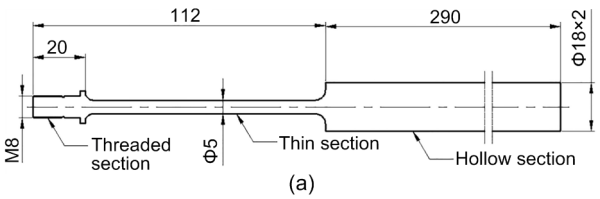

(a)

(b)

Fig. 2 Experimental tubes (unit: mm)

(a) Structural dimensions of a single tube; (b) A tube array

The experimental tube was made of 304 stainless steel and consisted of a threaded section, thin section, and hollow section (Fig. 2). The threaded section was connected to a tube sheet to secure the tube. The thin section was designed to reduce the natural frequency of the tube so as to achieve a critical flow velocity that was within the capability of the water pump and air compressor. The end of the hollow section was sealed with a small rubber plug to eliminate the influence of the fluid inside the tube on the vibration of the tube bundles. The circumference of the measured flexible tubes was surrounded by rigid tube bundles. In this way the influence of mutual movement of the tubes on the damping test could be avoided. In the experimental apparatus, the flexible tube was a cantilever beam with one end fixed and the other free, while the rigid tube was fixed at both ends.

There are generally four types of tube bundle arrangements in heat exchangers, namely, normal and rotated triangular, and normal and rotated square. Besides these arrangements, the pitch-to-diameter ratio was also considered in the experiments, giving a total of nine arrangement schemes of tube bundles (Table 2 and Fig. 3).

Table 2 Schemes of tube bundle arrangement

Pitch-to-diameter ratio	Arrangement			
	Normal square	Normal triangular	Rotated square	Rotated triangular
1.48	a	d	–	–
1.39	b	e	g	–
1.32	c	f	h	i

2.2 Measurement and calculation of parameters

To study the fluid-elastic instability of tube bundles, it is necessary to measure and calculate

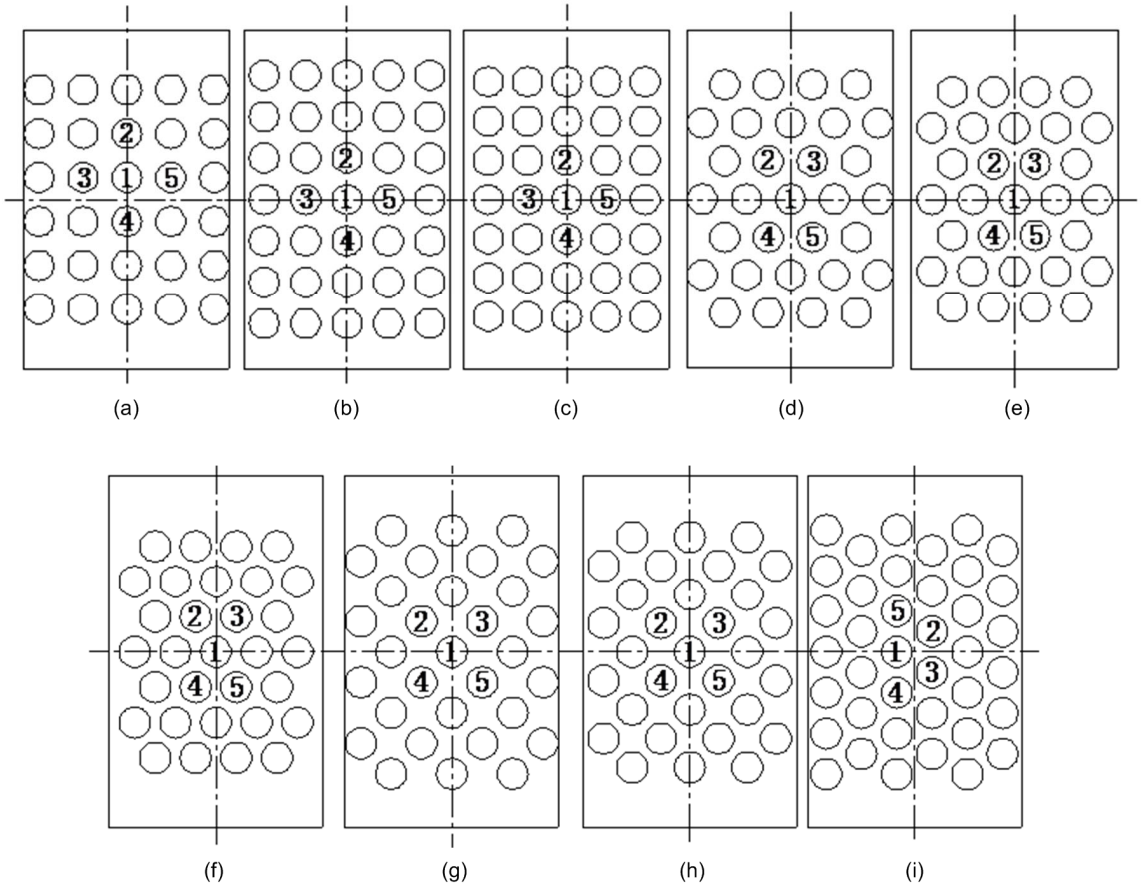

Fig. 3 Tube bundle arrangement schemes (a–i) listed in Table 2
Numbers indicate tubes that were tested

parameters such as flow velocity, void fraction, amplitude, frequency, and damping ratio. The flow rates of the liquid and gas were measured by an electromagnetic flowmeter and a rotor flowmeter, respectively. The void fraction α was measured with the help of a dual conductivity probe. The available maximum conductivity difference measurement (CDM) void fraction was 50% in the present experiments due to the limited air flow supply. The first order natural frequency of the tube in still air was measured by a free vibration method. The average value was 12.619 Hz for the test tube. The first order natural frequency in two-phase flow was calculated by fast Fourier transform (FFT) of experimental results. The damping ratio was obtained using the half-power bandwidth method (Moran and Weaver, 2013). The measurement and calculation of flow velocity, hydrodynamic mass, and amplitude will be described in detail below.

2.2.1 Flow velocity

Pettigrew et al. (2005) found that there was almost no slip in the continuous flow between the tubes, which means the two phases had the same velocity. Since the measured CDM void fraction α takes into account the compressibility of the air, the free flow velocity V_0 was calculated as

$$V_0 = \frac{Q_l + Q_g}{S} = \frac{Q_l}{S(1-\alpha)}, \tag{3}$$

where Q_l is the volume flow rate of the water, Q_g is the modified volume flow rate of the air, and S is the cross-sectional area of the test section chamber. The pitch velocity V_p was calculated using the formulas listed in Table 3 according to the free flow velocity and the pitch-to-diameter ratio.

Table 3 Formulas for calculating pitch velocity (Pettigrew and Taylor, 1991)

Arrangement	Angle	Calculation formula
Normal square/ Normal triangular	90°/30°	$V_p = V_0 \frac{p/d}{p/d-1}$
Rotated square	45°	$V_p = \frac{V_0}{\sqrt{2}} \frac{p/d}{p/d-1}$
Rotated triangular	60°	$V_p = \frac{\sqrt{3}V_0}{2} \frac{p/d}{p/d-1}$

2.2.2 Hydrodynamic mass

The hydrodynamic mass is the equivalent mass of the vibrating fluid outside the tube. Pettigrew et al. (1989a) derived a formula for calculating the hydrodynamic mass in a two-phase cross flow according to that for a two-phase axial flow (Carlucci and Brown, 1983), as follows:

$$m_h = m_l\left[\left(f_g/f\right)^2 - 1\right], \tag{4}$$

where m_h is the hydrodynamic mass per unit length, m_l is the mass of tube per unit length, f_g is the vibration frequency of tube in the gas, and f is the vibration frequency of tube in the two-phase flow.

2.2.3 Amplitude

To calculate the amplitude of the flexible tube, we used a simplified model (Fig. 4) which assumes that the fluid force acting on the tube is uniformly distributed and the effect of the fluid on the thin section is neglected. The hollow section can be regarded as a rigid body compared with the thin section, as the inertia moment of the hollow section is about 107 times that of the thin section, and the displacement y of its free end is

$$y = -\frac{l_2\left(4l_2^2 + 9ll_2 + 6l^2\right)}{6r\left(l + 2l_1\right)}\varepsilon, \tag{5}$$

where l is the length of the tube, l_1 is the distance between the strain gauge and the variable cross section, l_2 is the length of the thin section, r is the radius of the thin section, and ε is the strain. The tube amplitude can be derived from the root mean square of its end displacement, which is calculated as

$$A_{rms} = \sqrt{\frac{1}{N}\sum_{i=1}^{N}\left(y_i - \bar{y}\right)^2}, \tag{6}$$

where N is the number of samples, and y_i is the static shift of each sample. The average amplitude $\bar{y}$ in the formula represents the static shift of the tube in the direction of lift or drag caused by the fluid force exerted on the tube.

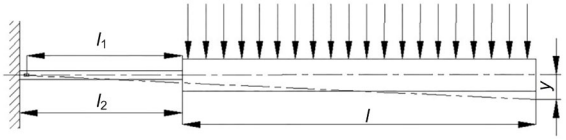

Fig. 4 Simplified model for calculating the amplitude of a flexible tube

3 Results and discussion

3.1 Damping characteristics

If the distribution of the local void fraction, which is a function of time and space, is not uniform around the tube, it will cause fluctuation of the additional mass of the tube and hence lead to a change of the natural frequency of the tube. This phenomenon called "frequency drift" would widen the bandwidth around the natural frequency in the spectrum curve, which in turn may result in enlargement of the damping ratio of the flexible tube bundle calculated by the half power bandwidth method. Consequently, the damping ratios referred to herein were all obtained in a single flexible tube surrounded by rigid tube bundles, consistent with the suggestion of Mitra (2005). Moreover, to avoid the effect of fluid-elastic instability on the damping test, the damping ratios in this study were set corresponding to the pitch velocity at one-half critical velocity (Pettigrew et al., 1989b).

3.1.1 Damping in lift and drag directions

When a fluid flows across a tube bundle, a drag force acting on the tube is generated along the flow direction, while a lift force is generated perpendicular to the flow direction. Generally, the damping ratios in the two directions are different. Taking tube 4 (number shown in Fig. 3a) in the normal square tube bundles with a pitch-to-diameter ratio of 1.48 as an example, the damping ratio curve versus pitch velocity is plotted in Fig. 5. The plot indicates that the

damping ratio in the lift direction was significantly smaller than that in the drag direction. Also, when the pitch velocity exceeded a certain value, the damping ratio decreased in the lift direction and increased in the drag direction. Note that the experimental results of Pettigrew et al. (1989b) show that fluid-elastic instability of tube bundles usually occurs earlier in the lift direction, so in the absence of exceptional circumstances, the damping ratio below refers to that in the lift direction.

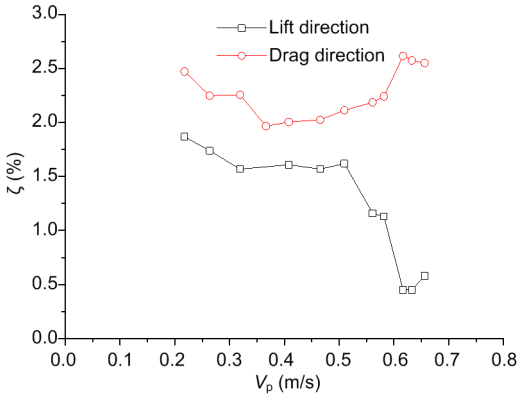

Fig. 5 Damping ratio ζ in lift and drag directions versus pitch velocity V_p
Normal square; p/d=1.48; α=10%

3.1.2 Effect of volumetric void fraction on damping

The volumetric void fraction and damping ratio are two important parameters for fluid-elastic instability. The effects of the volumetric void fraction on the damping ratio for different tube arrangements and pitch-to-diameter ratios are shown in Fig. 6. The damping ratio of the normal square and normal triangular tube bundles increased first and then decreased with increasing void fraction in the range of void fractions considered in this study. When it comes to the rotated square and rotated triangular arrangements, the damping ratio increased with increasing void fraction and there was no obvious decline. The reason for this difference may be related to the fluid flow path in different arrangements.

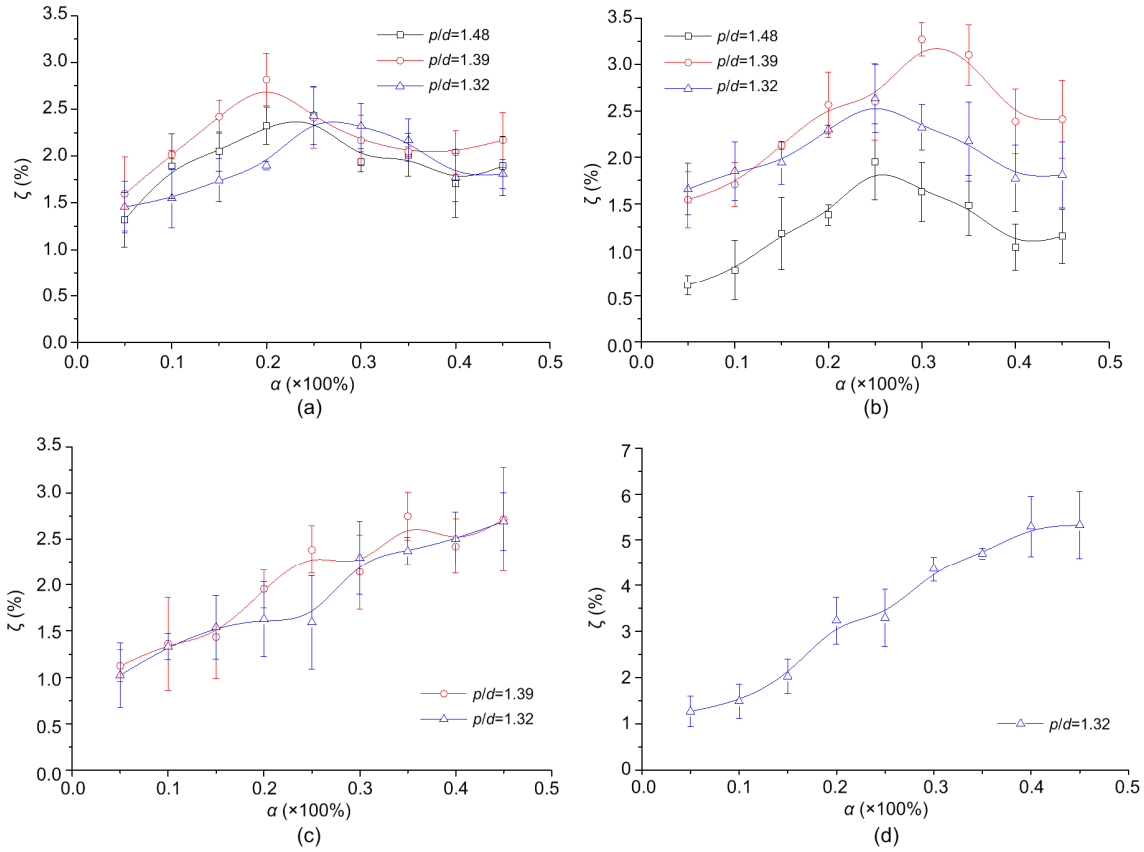

Fig. 6 Effect of the volumetric void fraction on the damping ratio
(a) Normal square; (b) Normal triangular; (c) Rotated square; (d) Rotated triangular

3.1.3 Effect of tube bundle arrangement on damping

Taking the middle tube 1 (number shown in Fig. 3) in the four tube bundle arrangements with a pitch-to-diameter ratio of 1.32 as an example, the curves of the damping ratio versus the void fraction are plotted in Fig. 7. The arrangement mode had little effect on the damping ratio when the void fraction was less than 15%, whereas the damping ratios differed obviously for different arrangements when the void fraction was higher than 15%, and the damping ratio was the biggest for the rotated triangular arrangement. This is because in a rotated triangular arrangement there are more tubes for the same cross section, so the gap between the tubes is the smallest. Thus, the interaction between the fluid flow and the tubes is greater, resulting in a larger damping.

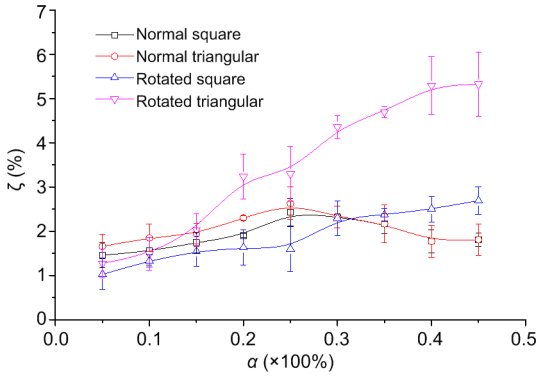

Fig. 7 Damping ratios under different arrangements with a pitch-to-diameter ratio of 1.32

3.2 Vibration characteristics

Fluid-elastic instability is one of the most destructive excitation mechanisms. To avoid damage due to the vibration of tube bundles, it is essential to determine the critical flow velocity. Fig. 8 shows the relationship between the pitch velocity and the root mean square amplitude of normal square tube bundles with a pitch-to-diameter ratio of 1.48 when the void fraction was 5%. The amplitude of the tube bundles increased sharply when the flow velocity reached a certain value, indicating the onset of fluid-elastic instability. In this study, the critical flow velocity was defined as the pitch velocity corresponding to the intersection of the two fitting lines before and after the occurrence of fluid-elastic instability. For those tube bundles whose vibration curves had no obvious slope change similar to that in Fig. 8 (Sim and Park, 2010), the critical velocity was defined as the pitch velocity at which the root mean square amplitude began to increase significantly.

To compare the vibration characteristics of tube bundles in the lift and drag directions, the curve of the root mean square amplitude of normal square tube bundles with p/d=1.48 is plotted in Fig. 9 against the pitch velocity. The critical velocity of the tube bundles in the lift direction was smaller than that in the drag direction. This phenomenon means that tube bundles first underwent fluid-elastic instability in the lift direction, i.e. the tube bundles were more susceptible to damage in the lift direction. Based on the above, the subsequent discussion focuses mainly on the fluid-elastic instability of tube bundles in the lift direction.

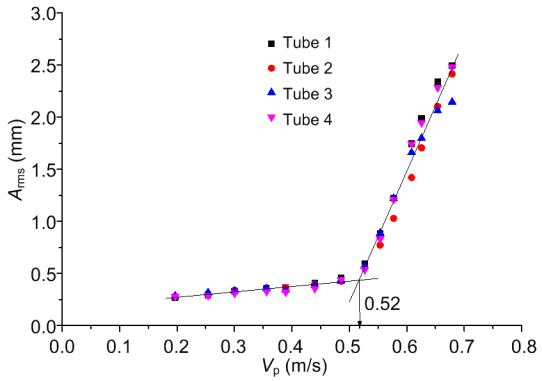

Fig. 8 Linear fitting of root mean square amplitude versus pitch velocity

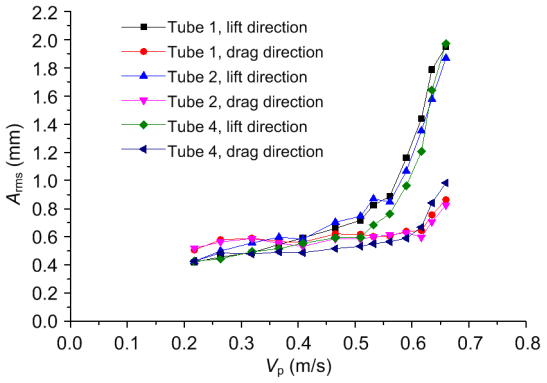

Fig. 9 Root mean square amplitude of tube bundles versus pitch velocity
Normal square, p/d=1.48, α=10%

3.3 Fluid-elastic instability

3.3.1 Influencing factors

The pitch-to-diameter ratio and tube arrangement are two important structural factors that greatly affect the fluid-elastic instability of heat exchanger tube bundles. Stability maps of normal square and normal triangular tube bundles are plotted in Fig. 10 to investigate the effect of the pitch-to-diameter ratio on fluid-elastic instability. Since the slope of the fitting line, i.e. the exponent n in the Connors correlation, was close to 0.5, the exponent was directly taken as 0.5 to facilitate a comparison of the instability constant K between different tube bundle arrangements. The instability constants K obtained from the fitting lines are summarized in Table 4. The effect of the pitch-to-diameter ratio on fluid-elastic instability appears to have no evident regularity for normal square and normal triangular arrangements.

To further study the effect of the tube bundle arrangement on fluid-elastic instability, the dimensionless velocity and mass damping parameters of four tube bundle arrangements with p/d=1.32 were tested and calculated experimentally. The stability map is also plotted in Fig. 11. For the rotated square and rotated triangular tube bundles, the Connors exponent was 0 at low mass damping and 0.5 at high mass damping. The fitted values of the instability constant K are listed in Table 5. The instability constants corresponding to the two normal bundles (referring to normal square and normal triangular bundles) were significantly larger than those corresponding to the two rotated bundles (referring to rotated square and rotated triangular bundles). This means the two

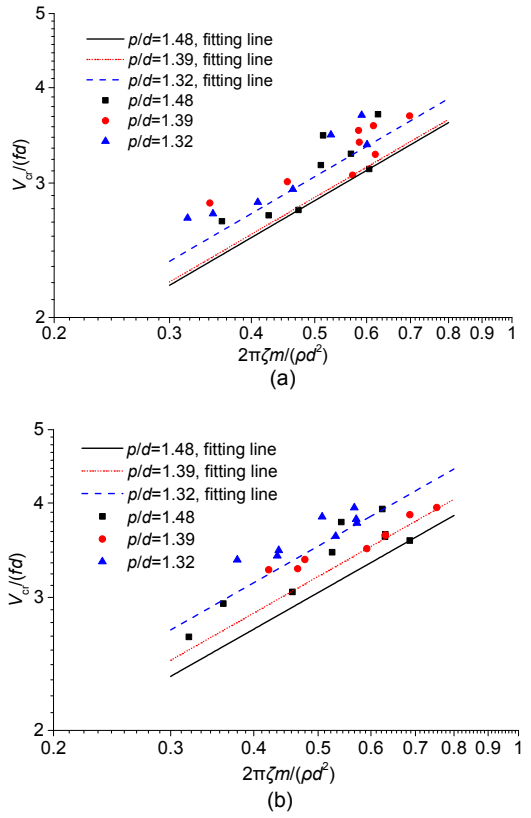

Fig. 10 Stability maps of tube bundles with different pitch-to-diameter ratios
(a) Normal square; (b) Normal triangular

Table 4 Instability constants K for normal square and normal triangular arrangements

Arrangement	p/d	Instability constant K	Exponent n
Normal square	1.48	4.03	0.5
	1.39	4.07	0.5
	1.32	4.33	0.5
Normal triangular	1.48	4.31	0.5
	1.39	4.52	0.5
	1.32	4.96	0.5

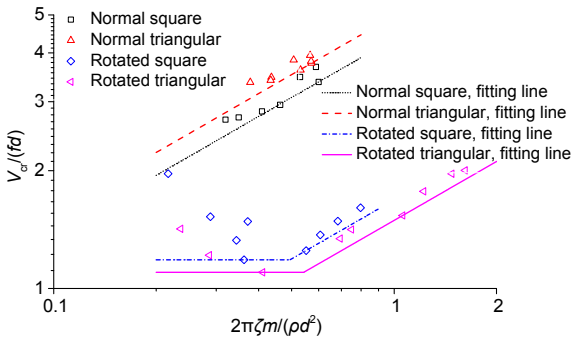

Fig. 11 Stability map of four tube bundle arrangements with p/d=1.32

Table 5 Instability constants K for four tube bundle arrangements with p/d=1.32

Arrangement		Instability constant K	Exponent n
Normal square		4.35	0.5
Normal triangular		4.98	0.5
Rotated square	$2\pi\zeta m/(\rho d^2)\leq 0.50$	1.18	0.0
	$2\pi\zeta m/(\rho d^2)>0.50$	1.68	0.5
Rotated triangular	$2\pi\zeta m/(\rho d^2)\leq 0.54$	1.10	0.0
	$2\pi\zeta m/(\rho d^2)>0.54$	1.49	0.5

rotated bundles were more prone to fluid-elastic instability than the two normal bundles. The difference is probably related to the fluid flow path formed by the tube bundles.

3.3.2 Design guidelines

A stability map based on the dimensionless flow velocity and mass damping parameter generally contains two unstable zones, and the transition between the two zones corresponds to the transition between continuous flow and intermittent flow. However, the unstable behavior of tube bundles is different in these two flows. According to Pettigrew and Taylor (1994), operation in intermittent flow should be avoided for heat exchanger tube bundles, as it may lead to a lower critical flow velocity. In addition, Pettigrew et al. (2001) pointed out that a void fraction below 80% is the critical condition to ensure continuous flow. The void fraction measured by the dual conductivity probe in this study, whose maximum value was 50%, was much lower than the critical void fraction, and thus the two-phase flow in our experiments could be regarded as continuous flow.

To obtain recommended values of instability constants with wide adaptability and simplicity, it is essential to classify the experimental data according to the influence of the variables on the fluid-elastic instability. Comparing Fig. 10 with Fig. 11, we conclude that the tube bundle arrangement has the greatest influence on the fluid-elastic instability compared with other geometric features of the tube bundle. Note that there is a big difference between the stability maps of the two normal bundles and the two rotated bundles; therefore, these two types can be classified into different groups. Based on the above classification, the stability map shown in Fig. 12 was plotted, in which the recommended line refers to the line fitted by the point at the lowest boundary. The values of the instability constant K determined by the recommended line in Fig. 12 are summarized in Table 6. For the two normal bundles, the value of K is 4.0, which is apparently larger than that calculated by Eq. (2). For the two rotated bundles, the value of K is 1.1 when $2\pi\zeta m/(\rho d^2)\leq 0.54$ and 1.5 when $2\pi\zeta m/(\rho d^2)>0.54$; however, the K values calculated by Eq. (2) range from 2.3 to 3.0 when the pitch-to-diameter ratio is 1.32 or 1.48, which are larger than the two recommended values proposed in this study. Consequently, it is not reasonable to ignore the effect of tube bundle arrangement on the instability constant, as in Eq. (2).

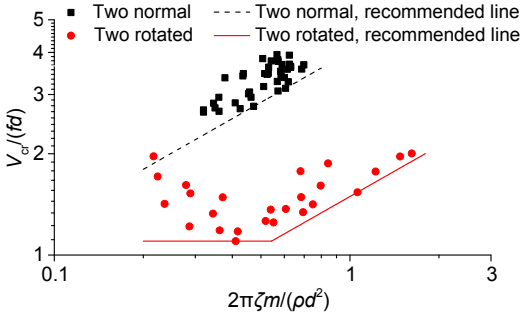

Fig. 12 Determination of instability constants K for four tube bundle arrangements with different pitch-to-diameter ratios

Table 6 Recommended values of the instability constant K

Arrangement		Recommended value of K
Normal square/Normal triangular		4.0
Rotated square/ Rotated triangular	$2\pi\zeta m/(\rho d^2)\leq 0.54$	1.1
	$2\pi\zeta m/(\rho d^2)>0.54$	1.5

3.3.3 Comparison with previous research results

To verify the validity of the recommended values of the instability constants, the data in Table 6 were compared with the results of previous studies. Ricciardi et al. (2011) carried out experimental research on the fluid-elastic instability of normal triangular tube bundles exposed to air-water cross flow. The minimum value of the instability constant was 5.1, which is greater than 4.0 recommended in Table 6. The fluid-elastic instability of normal square tube bundles with p/d=1.46 in a steam-water cross flow was studied by Hirota et al. (2002). When the void fraction was less than 50%, the instability constants obtained were all larger than 4.0. Moreover, Feenstra et al. (2002) found that for rotated triangular tube bundles with p/d=1.44, the instability constant was 2.0 when a two-phase cross flow of Freon-11 was a bubbly flow, which was obviously greater than the maximum value of the instability constant recommended in this study. According to the above analysis, for the four tube bundle arrangements with pitch-to-diameter ratios between 1.32 and 1.48, the

recommended values of the instability constants in Table 6 represent a lower bound of the measured data in the present set of tests.

To further illustrate the validity of the values of the instability constants recommended in this paper, the results of the present experiment and of previous studies were plotted in the same stability map (Fig. 13). For the two normal bundles (Fig. 13a), the instability constant determined by Pettigrew et al. (1989b) and Pettigrew and Taylor (2009) was 3.4, some 15% lower than the value recommended here. This is because the range of their data was relatively wide, resulting in a downward shift of the corresponding fitting line. The experimental data of Feenstra et al. (2003) were in good agreement with our data. Thus, when the void fraction was less than 50%, the instability constant for normal square and normal triangular tube bundles was 4.0, which was proved to be reliable.

The recommended value of the instability constant according to the data of Pettigrew et al. (1989b, 1995, 2002) and Feenstra et al. (2002) was 3.0 for the two rotated bundles (Fig. 13b), which was quite different from the results in this study. The void fraction measurement method used in this study was different from that adopted by Pettigrew et al. (1989b, 1995, 2002) and Feenstra et al. (2002). The dual conductivity probe measurement method, namely the CDM model method, was adopted in this study, while Feenstra et al. (2002) used the gamma densitometer measurement method, also known as the radiation attenuation determination (RAD) model method, both of which are direct measurement methods. The ideal homogeneous equilibrium model (HEM) was employed by Pettigrew et al. (1989b, 1995, 2002) to obtain the void fraction. The difference between void fractions measured by the HEM and direct measurement methods is that the HEM assumes the two phases are well mixed and flow at the same velocity. Hence, the HEM usually predicts a higher void fraction than direct measurement methods, and therefore indicates a lower average density. Since density is in the denominator of the calculation formula of the mass damping parameter, a lower density leads to a higher mass damping parameter in the HEM, which results in an upward shift of the recommended line of the instability constant. However, although in both of this study and Feenstra et al. (2002) direct measurement methods were adopted to obtain the void fraction, the selected type of flow velocity was different. The pitch velocity based on the CDM model was used in this study, while Feenstra et al. (2002) considered the slip between two-phase flows and adopted the interface velocity. This is the reason why the line proposed by Feenstra et al. (2002) was above that proposed in this study.

In addition, the distributions of two dimensionless parameters obtained by Feenstra et al. (2002) on the basis of the interface velocity were relatively concentrated so that there was no obvious linear trend. Therefore, it is doubtful whether the Connors correlation is suitable for the analysis of fluid-elastic instability based on the interface velocity.

Based on the above analysis, we conclude that the proposed method based on the CDM model to

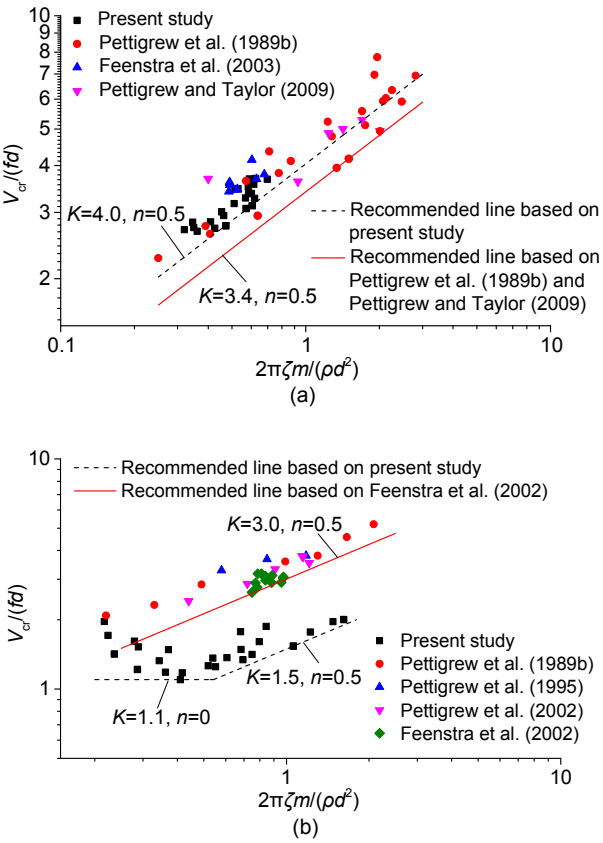

Fig. 13 Comparison of instability constants determined in different studies

(a) Normal square and normal triangular; (b) Rotated square and rotated triangular

modify the pitch velocity is feasible for developing the design guidelines of the fluid-elastic instability of tube bundles subjected to two-phase cross flow.

4 Conclusions

Fluid-elastic instability is the major cause of vibration failure of heat exchanger tube bundles. In view of the inconsistency of design guidelines for fluid-elastic instability subjected to two-phase cross flow, the effects of the void fraction, pitch-to-diameter ratio, and tube bundle arrangement on the damping characteristics, vibration characteristics, and fluid-elastic instability of tube bundles were investigated experimentally using an air-water system. Instability constants were recommended in the case of void fractions of less than 50%, and their validity was verified. The main conclusions from this study are as follows:

1. The damping ratio in the lift direction was obviously smaller than that in the drag direction, and was significantly affected by the void fraction. Generally, with increasing void fraction, the damping ratio of normal square and normal triangular tube bundles first increased and then decreased, while the damping ratio of rotated square and rotated triangular tube bundles increased monotonically. The damping ratio of the rotated triangular tube bundle was the largest among the four tube bundle arrangements under the same operating and geometric conditions.

2. The tube bundle was more prone to fluid-elastic instability in the lift direction than in the drag direction. The normal square and normal triangular tube bundles with a pitch-to-diameter ratio of 1.48 were more susceptible to fluid-elastic instability than those with a pitch-to-diameter ratio of 1.32. The order of stability of the four tube bundle arrangements with the same pitch-to-diameter ratio from high to low was: normal triangular, normal square, rotated square, rotated triangular. Therefore, to avoid fluid-elastic instability, the normal triangular arrangement with a small pitch-to-diameter ratio is recommended for large shell-and-tube heat exchangers subjected to two-phase cross flow.

3. Based on the classification of tube bundle arrangements, a method to determine the instability constant was proposed. The value of the instability constant K was 4.0 for the two normal bundles, and 1.1 for the two rotated bundles when $2\pi\zeta m/(\rho d^2)\leq 0.54$ and 1.5 when $2\pi\zeta m/(\rho d^2)>0.54$. A comparison with other research results indicated that the instability constants proposed in this study are reasonable and reliable for two-phase cross flow when the void fraction is less than 50%.

Contributors

Ning SUN wrote the first draft of the manuscript and revised the final version. Rui-jia CHENG processed and analyzed the experimental data. Ya-nan ZHANG conducted the experimental research. Bao-qing LIU supervised and led the plan and implementation of research activities. Bengt SUNDEN put forward the objective of investigation and improved the experimental research.

Conflict of interest

Ning SUN, Rui-jia CHENG, Ya-nan ZHANG, Bao-qing LIU, and Bengt SUNDEN declare that they have no conflict of interest.

References

Álvarez-Briceño R, Kanizawa FT, Ribatski G, et al., 2017. Updated results on hydrodynamic mass and damping estimations in tube bundles under two-phase crossflow. *International Journal of Multiphase Flow*, 89:150-162. https://doi.org/10.1016/j.ijmultiphaseflow.2016.09.022

Álvarez-Briceño R, Kanizawa FT, Ribatski G, et al., 2018. Validation of turbulence induced vibration design guidelines in a normal triangular tube bundle during two-phase crossflow. *Journal of Fluids and Structures*, 76:301-318. https://doi.org/10.1016/j.jfluidstructs.2017.10.013

Axisa F, Villard B, Gibert RJ, et al., 1984. Vibration of tube bundles subjected to air-water and steam-water cross-flow. Preliminary results on fluid-elastic instability. Proceedings of ASME Symposium on Flow-induced Vibrations, p.269-284.

Carlucci LN, Brown JD, 1983. Experimental studies of damping and hydrodynamic mass of a cylinder in confined two-phase flow. *Journal of Vibration, Acoustics, Stress, and Reliability in Design*, 105(1):83-89. https://doi.org/10.1115/1.3269073

Chung HJ, Chu IC, 2005. Fluid elastic instability of rotated square array tube bundle in two-phase cross-flow. Proceedings of ASME 2005 Pressure Vessels and Piping Conference, p.627-634. https://doi.org/10.1115/PVP2005-71637

Connors HJ, 1970. Fluid-elastic vibration of tube arrays excited by cross-flow. Proceedings of ASME Winter Annual Meeting, p.42-56.

Desai SR, Pavitran S, 2018. The effect of fin pitch on fluid

elastic instability of tube arrays subjected to cross flow of water. *Journal of the Institution of Engineers (India): Series C*, 99(1):53-61.
https://doi.org/10.1007/s40032-016-0332-z

Feenstra PA, Weaver DS, Judd RL, 2002. Modelling two-phase flow-excited damping and fluidelastic instability in tube arrays. *Journal of Fluids and Structures*, 16(6):811-840.
https://doi.org/10.1006/jfls.2002.0442

Feenstra PA, Weaver DS, Nakamura T, 2003. Vortex shedding and fluidelastic instability in a normal square tube array excited by two-phase cross-flow. *Journal of Fluids and Structures*, 17(6):793-811.
https://doi.org/10.1016/S0889-9746(03)00024-0

Hirota K, Nakamura T, Kasahara J, et al., 2002. Dynamics of an in-line tube array subjected to steam–water cross-flow. Part III: fluidelastic instability tests and comparison with theory. *Journal of Fluids and Structures*, 16(2):153-173.
https://doi.org/10.1006/jfls.2001.0408

Liu BQ, Cheng RJ, Zhang YN, et al., 2018. Experimental research on fluid-elastic instability in tube bundles subjected to air-water cross flow. *Nuclear Science and Engineering*, 189(3):290-300.
https://doi.org/10.1080/00295639.2017.1394084

Liu LY, Xu W, Guo K, et al., 2018. The fluid elastic instability of concentric arrays of tube bundles subjected on cross flow. Proceedings of ASME 2018 Pressure Vessels and Piping Conference.
https://doi.org/10.1115/PVP2018-84352

Mitra D, 2005. Fluid-elastic Instability in Tube Arrays Subjected to Air-water and Steam-water Cross-flow. PhD Thesis, University of California at Los Angeles, Los Angeles, USA.

Mitra D, Dhir VK, Catton I, 2009. Fluid-elastic instability in tube arrays subjected to air-water and steam-water cross-flow. *Journal of Fluids and Structures*, 25(7):1213-1235.
https://doi.org/10.1016/j.jfluidstructs.2009.07.002

Moran JE, Weaver DS, 2013. On the damping in tube arrays subjected to two-phase cross-flow. *Journal of Pressure Vessel Technology*, 135(3):030906.
https://doi.org/10.1115/1.4023421

Pettigrew MJ, Taylor CE, 1991. Fluidelastic instability of heat exchanger tube bundles: review and design recommendations. *Journal of Pressure Vessel Technology*, 113(2):242-256.
https://doi.org/10.1115/1.2928752

Pettigrew MJ, Taylor CE, 1994. Two-phase flow-induced vibration: an overview (survey paper). *Journal of Pressure Vessel Technology*, 116(3):233-253.
https://doi.org/10.1115/1.2929583

Pettigrew MJ, Taylor CE, 2009. Vibration of a normal triangular tube bundle subjected to two-phase Freon cross flow. *Journal of Pressure Vessel Technology*, 131(5):051302.
https://doi.org/10.1115/1.3147985

Pettigrew MJ, Taylor CE, Kim BS, 1989a. Vibration of tube bundles in two-phase cross-flow: part 1—hydrodynamic mass and damping. *Journal of Pressure Vessel Technology*, 111(4):466-477.
https://doi.org/10.1115/1.3265705

Pettigrew MJ, Tromp JH, Taylor CE, et al., 1989b. Vibration of tube bundles in two-phase cross-flow: part 2—fluidelastic instability. *Journal of Pressure Vessel Technology*, 111(4):478-487.
https://doi.org/10.1115/1.3265706

Pettigrew MJ, Taylor CE, Jong JH, et al., 1995. Vibration of a tube bundle in two-phase Freon cross-flow. *Journal of Pressure Vessel Technology*, 117(4):321-329.
https://doi.org/10.1115/1.2842130

Pettigrew MJ, Taylor CE, Kim BS, 2001. The effects of bundle geometry on heat exchanger tube vibration in two-phase cross flow. *Journal of Pressure Vessel Technology*, 123(4):414-420.
https://doi.org/10.1115/1.1388236

Pettigrew MJ, Taylor CE, Janzen VP, et al., 2002. Vibration behavior of rotated triangular tube bundles in two-phase cross flows. *Journal of Pressure Vessel Technology*, 124(2):144-153.
https://doi.org/10.1115/1.1462045

Pettigrew MJ, Zhang C, Mureithi NW, et al., 2005. Detailed flow and force measurements in a rotated triangular tube bundle subjected to two-phase cross-flow. *Journal of Fluids and Structures*, 20(4):567-575.
https://doi.org/10.1016/j.jfluidstructs.2005.02.007

Ricciardi G, Pettigrew MJ, Mureithi NW, 2011. Fluidelastic instability in a normal triangular tube bundle subjected to air-water cross-flow. *Journal of Pressure Vessel Technology*, 133(6):061301.
https://doi.org/10.1115/1.4004562

Sim WG, Park MY, 2010. Fluid-elastic instability of normal square tube bundles in two-phase cross flow. Proceedings of the 18th International Conference on Nuclear Engineering, p.7-14.
https://doi.org/10.1115/ICONE18-29037

Violette R, Pettigrew MJ, Mureithi NW, 2006. Fluidelastic instability of an array of tubes preferentially flexible in the flow direction subjected to two-phase cross flow. *Journal of Pressure Vessel Technology*, 128(1):148-159.
https://doi.org/10.1115/1.2138064

Weaver DS, Fitzpatrick JA, 1988. A review of cross-flow induced vibrations in heat exchanger tube arrays. *Journal of Fluids and Structures*, 2(1):73-93.
https://doi.org/10.1016/S0889-9746(88)90137-5

中文概要

题　目：两相横向流中管束弹性不稳定性的设计准则

目　的：流体弹性不稳定性是引起换热器管束振动失效的

最主要原因。鉴于目前有关两相横向流诱发管束弹性不稳定性的设计准则尚无一致结论，本文采用空气-水两相流体系，考察不同参数条件下换热器管束的弹性不稳定性。

创新点： 1. 从避免发生弹性不稳定性的角度，确定适宜的管束排列方式和节径比；2. 建立基于 Connors 准则的不稳定常数的确定方法，并提出新的推荐值。

方　法： 1. 实验研究两相流的流动条件和管束的几何特征对管束阻尼、振动特性及弹性不稳定性的影响；2. 采用建立稳定区图的方法确定不稳定常数的推荐值；3. 通过与其他研究成果的对比分析，验证本文推荐的不稳定常数的合理性和可靠性。

结　论： 1. 相比于阻力方向，升力方向上的阻尼比更小，也更易发生弹性失稳。2. 四种排列管束的稳定性从高到低依次为：正三角形、正方形、转置正方形、转置正三角形。3. 对于正方形和正三角形排列管束，推荐不稳定常数为 4.0；对于转置正方形和转置正三角形排列管束，当质量阻尼参数小于或等于 0.54 时，推荐不稳定常数为 1.1，反之，则推荐不稳定常数为 1.5。

关键词： 管束；弹性不稳定性；两相横向流；设计准则